AIP | The Journal of Chemical Physics

Impedance measurements on a DNA junction

Sungmin Hong, Luis A. Jauregui, Norma L. Rangel, Huan Cao, B. Scott Day, Michael L. Norton, Alexander S. Sinitskii, and Jorge M. Seminario

Citation: The Journal of Chemical Physics **128**, 201103 (2008); doi: 10.1063/1.2937127
View online: http://dx.doi.org/10.1063/1.2937127
View Table of Contents: http://scitation.aip.org/content/aip/journal/jcp/128/20?ver=pdfcov
Published by the AIP Publishing

Impedance measurements on a DNA junction

Sungmin Hong,[1,2] Luis A. Jauregui,[1,3] Norma L. Rangel,[1,4] Huan Cao,[5] B. Scott Day,[5] Michael L. Norton,[5] Alexander S. Sinitskii,[6] and Jorge M. Seminario[1,4,7,a)]
[1]*Department of Chemical Engineering, Texas A&M University, College Station, Texas 77843, USA*
[2]*Department of Biomedical Engineering, Texas A&M University, College Station, Texas 77843, USA*
[3]*Facultad de Ingeniería Eléctrica y Electrónica, Universidad Nacional de Ingeniería, Lima 25, Peru*
[4]*Materials Science and Engineering Graduate Program, Texas A&M University, College Station, Texas 77843, USA*
[5]*Department of Chemistry, Marshall University, Huntington, West Virginia 25755, USA*
[6]*Department of Chemistry, Rice University, Houston, Texas 77005, USA*
[7]*Department of Electrical and Computer Engineering, Texas A&M University, College Station, Texas 77843, USA*

(Received 31 March 2008; accepted 6 May 2008; published online 29 May 2008)

1 μm double-stranded DNA molecules are immobilized between pairs of gold and pairs of platinum microelectrodes with gaps of 0.4 and 1 μm, respectively, and their electrical characteristics are determined under the application of constant and sinusoidal bias voltages. Due to their extremely high impedance for constant voltage bias, the samples of DNA are excellent insulators; however, their impedances show strong frequency dependence in the range of 10 Hz–7.5 MHz. Favorable response in the gold electrodes is attributed to the higher ability of DNA molecules to bridge the narrower gold electrode gaps in contrast to that in the wider platinum junctions. © *2008 American Institute of Physics*. [DOI: 10.1063/1.2937127]

There has been considerable interest in developing electrical circuits with DNA.[1,2] DNA electronics take advantage of the tunneling and quantized capacitance in the phosphorus bridges and base-pair hydrogen bonds.[3] Thus, DNA electric circuits will be able to provide benefits in terms of miniaturization, low power consumption, high efficiency, and low heat generation.[4] A significant amount of research has been performed in the past decade on DNA-based field effect transistors[5] and DNA electronic sensors.[6] Singh *et al.* reported low frequency DNA devices such as a transistors[7] that reached a maximum channel current of 1.8 μA for a gate voltage of 10 V at 120 KHz. Subramanyam *et al.* reported low dielectric loss values ranging from 0.11 dB at 10 GHz to 0.5 dB at 30 GHz in DNA thin films.[8] Furthermore, DNA has been used to fabricate organic light-emitting diodes using thin film techniques[9] and electro-optic waveguide modulators using DNA biopolymers.[10]

Electron transfer through DNA molecules has been studied intensely in recent years. There have been many attempts to reveal the electrical nature of DNA using various methods such as radiochemical,[11] electrochemical,[12] colorimetric,[13] and chemiluminescent methods.[14] DNA electrical properties have also been obtained from conductance measurements of DNA using an 18 base-pair double-stranded DNA,[15] from the resistance measurement of DNA trapped by electrophoresis methods,[16] and from temperature dependent conduction measurements.[17] Furthermore, research on DNA conductance reported metallic,[18] insulating,[19] semiconducting,[20] and even superconducting[21] behaviors. This does suggest that electron transfer through DNA is very sensitive to the experimental environment thus making experimental results a controversial issue. The electrical behavior of DNA shows different results depending on DNA sequence[22] due to the ionic conduction of any residual buffer used in sample preparation.[23] Salt trapped between DNA molecules was reported as a possibility to increase conductance.[19] While several experiments[24–26] have been performed to characterize the steady-state direct current (dc) current-voltage (*I-V*) properties of DNA, only a small number of experiments[27,28] have focused on alternating current (ac) characteristics of DNA.

We have recently developed computational techniques to transmit signals in the terahertz domain through DNA and other biological molecules[29–38] as well as techniques to develop architectures that make use of molecular devices.[39–41] In the present work, we focus our study in the ac characteristics of DNA because any useful behavior of molecules as devices would need to deal with ac signals. We use 1 μm long DNA attached to multithiol terminated G3 polyamidoamine dendrimers to interconnect to the two metal electrodes.

Two types of chips are used to measure DNA impedance. Chip 1 consists of 20 pairs of gold electrodes, each pair with 400 nm gaps fabricated by standard electron-beam lithography and lift-off process (Fig. 1). Layers of 20 nm gold and 1 nm titanium are deposited on SiO_2/Si substrates. Chip 2 consists of microlithographically fabricated interdigitated microsensor electrodes.[42] Borosilicate glass chip consisted of one platinum electrode with five parallel lines at each end. Each line is 3 mm long and 2 μm wide, separated by 1 μm wide free spaces, as shown in Fig. 1 from a Nanoscope IIIa-Multimode atomic force microscope.[43]

Randomly sequenced double-stranded DNA ~1 μm long (3167 base pairs) is modified with multithiol dendrimer

a)Electronic mail: seminario@tamu.edu.

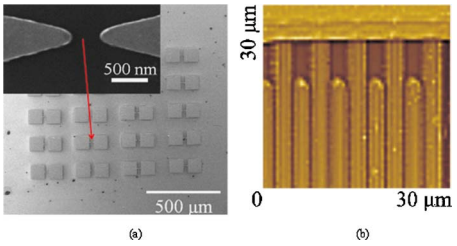

FIG. 1. (Color online) (a) SEM image of the gold electrodes with finger-shaped gap of ~400 nm shown in the inset. (b) AFM image of the 2 μm width fork-shaped platinum electrodes and gaps of 1 μm. *x*- and *y*-ranges go from 0 to 30 μm, and the *z*-range, perpendicular to the plane of the figure, goes from 0 (darkest) to 30 nm (lightest).

at both ends to increase connectivity to the gold electrodes. The DNA solution is diluted to 1:4 ratio with 25 mM EDTA buffer solution (pH=7.4). The final concentration is ~17 ng/μl. An additional 1 μl of 0.5*M* *N*-hydroxylamine is added for deacetylation of multithiolated groups. Then, the DNA solution is incubated for 30 min at room temperature. Before DNA exposure, the electrodes are carefully cleaned using ultrasonic bath with acetone for 2 min, and then washed with de-ionized (DI) water several times.

During DNA immobilization, the dielectrophoresis (DEP) method[44] is used to stretch DNA molecules. A DEP field of ac voltage of 2 $V_{p\text{-}p}$ is applied, which plays an important role to strengthen the DNA samples and increase the possibilities of having DNA samples connected to the electrodes. Then, 2 μl of DNA solution are poured onto the chip. For chip 1, the frequency of the field is set to 1 MHz for 1 h. For chip 2, we apply 1 MHz for the first time, a sweep of 100 Hz–1 kHz for the second time, and a constant field of 1 MHz for the third time, for 1 h each time. Once each chip has been treated accordingly, the electrodes are rinsed thoroughly with DI water. This process is repeated three times. Upon completion, the electrode is incubated at room temperature overnight. All these tasks are performed in a clean room facility.

In order to measure *I-V* characteristics, we use a probe station[45] that provides a vacuum of ~10^{-7} torr and it is equipped with an HP4145A semiconductor parameter analyzer[46] to control the applied voltage. The oscilloscope[47] (TDS 5104) and function generator[48] (AFG 3252) are used to measure the impedance of DNA molecules. The scanning electron microscope (JSM-6400, JEOL) is also employed for chip inspection. A Nanoscope IIIa-Multimode atomic force microscope[43] from Digital Instruments is used for the atomic force microscopy (AFM) analysis. All the samples are analyzed in close contact (tapping) mode in the AFM.

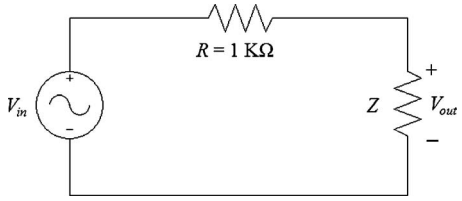

FIG. 2. Equivalent circuit for estimating the DNA impedance *Z* from the measurements of V_{in} and V_{out}.

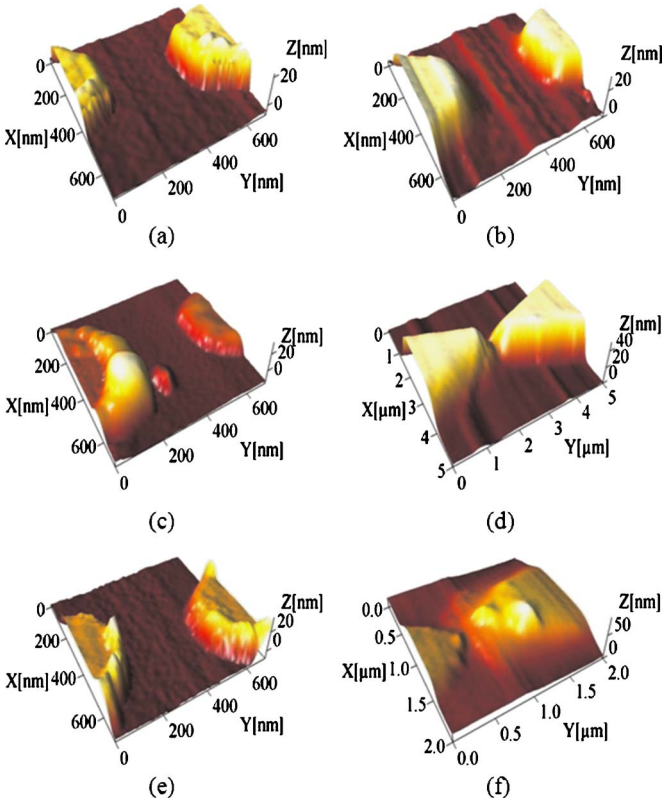

FIG. 3. (Color online) AFM images of the gold central electrodes: [(a) and (b)] electrode 3, [(c) and (d)] 13, and [(e) and (f)] 18 [(a), (c), and (e)] before and [(b), (d), and (f)] after DNA deposition.

We use our probe station,[45] function generator,[48] and oscilloscope[47] (0–1 GHz) to measure the frequency response of the chip. To derive the equations for impedance (Z), the circuit in Fig. 2 is used where the real and imaginary parts of Z are

$$\mathrm{Re}(Z) = \frac{0.5R\left(1 - \frac{V_{in}}{V_{out}}\cos\varphi\right)}{\frac{V_{in}}{V_{out}}\cos\varphi - 0.5\left(\left(\frac{V_{in}}{V_{out}}\right)^2 + 1\right)}, \tag{1}$$

$$\mathrm{Im}(Z) = \frac{-0.5R\left(\frac{V_{in}}{V_{out}}\sin\varphi\right)}{\frac{V_{in}}{V_{out}}\cos\varphi - 0.5\left(\left(\frac{V_{in}}{V_{out}}\right)^2 + 1\right)}, \tag{2}$$

respectively, thus the magnitude and phase of Z are given by

$$|Z| = \frac{R}{\sqrt{\left(\frac{V_{in}}{V_{out}}\right)^2 - \frac{2V_{in}}{V_{out}}\cos\varphi + 1}}, \tag{3}$$

$$\arg(Z) = \tan^{-1}\left(\frac{\frac{V_{in}}{V_{out}}\sin\varphi}{\frac{V_{in}}{V_{out}}\cos\varphi - 1}\right), \tag{4}$$

where $\varphi = \arg(V_{out}) - \arg(V_{in})$ is the phase difference between the output and input signals.

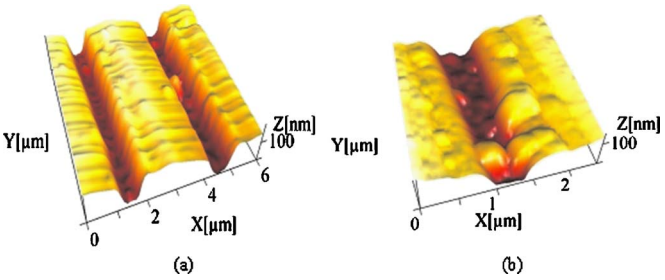

FIG. 4. (Color online) AFM images for the platinum electrode: (a) bare and (b) after DNA deposition.

The DNA sample attachment to the electrodes is suggested using AFM; the dc bias voltage yields the usual current response of the DNA material and now the impedance of DNA is measured using the ac bias. We expect that DNA conductivity should increase when the same DNA molecules from the DNA material are connected to both of their terminals. The AFM is operated in close contact mode with a scanning speed of 1 Hz. Figure 3 shows the AFM images of the central electrodes for chip 1; significant changes are observed in electrodes 13 and 18 after DNA deposition. Figure 4 shows the gaps filled with DNA chemically attached to the platinum electrodes through dendrimers.

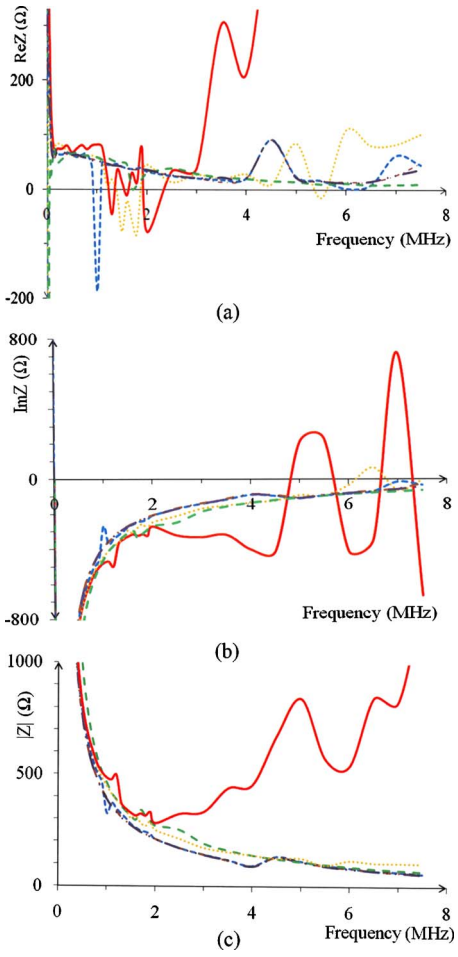

FIG. 5. (Color online) Impedance (in Ω's) plots for the gold electrodes (a) real and (b) imaginary parts, and (c) module. Bare gold (solid line, red) and after deposition of DNA on 1, 3, 8, 13, and 18 electrodes [dotted (orange), broken (blue), dashed (green), dashed dot line (brown), dashed dot dot (purple) lines, respectively].

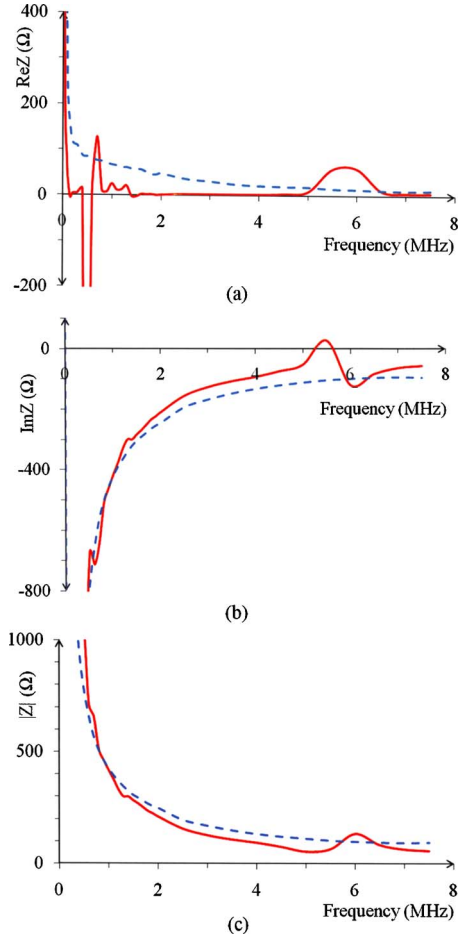

FIG. 6. (Color online) Impedance (Ω) plots for the platinum electrodes (a) real and (b) imaginary parts and (c) module. Solid line (red): bare electrode (solid, red line), after deposition of DNA (dashed blue line).

The *I-V* characteristics are measured to evaluate the electrical behavior of the junction before and after DNA deposition to the electrodes in chips 1 and 2. Measurements are performed at room temperature for both chips under the same conditions. The results for chip 1 are very noisy before and after DNA deposition with no perceptible current changes. For chip 1, the resistance is in the 50 TΩ range before and after DNA deposition. On the other hand, chip 2 shows resistances of 10 TΩ before DNA deposition and 2.5 TΩ after.

Figure 5 shows the noisy behavior of the chip impedance in the absence of DNA. The addition of DNA to the gold chip makes the components and thus the module of the impedance smoother and more stable. The impedance module shows a tendency to increase after 2 MHz but continuously decreases when the DNA is present. The imaginary component of the impedance (reactance) oscillates from inductive to capacitive behavior when there is no DNA on the chip, but it is smooth and practically keeps capacitive behavior when the DNA is placed on the chip.

Under the same conditions, on the platinum electrodes (chip 2), Fig. 6 shows an increase in resistance when compared to the bare platinum electrodes; also there is a parasitic inductance when DNA is not present on the chip and the

reactance shows a capacitive behavior in all the frequency range when DNA is present. In addition, the impedance module increases more when the DNA is present than when it is not, and as in the other cases, the response is smoother when the DNA is on the chip.

Due to the extremely high impedance for dc bias, the results of the experiment suggest that the *I-V* characteristics of the DNA system are similar to that of a good insulator. However, the impedance shows strong frequency dependence in both microelectrodes; it increases from 281 Ω at 2 MHz to 1302 Ω at 7.5 MHz for the gold junction and decreases from 232 Ω at 2 MHz to 97.6 Ω at 7.5 MHz for the platinum electrodes. Most likely, the size of the gap (1 μm) of the Pt junctions do not allow DNA molecules to bridge directly the two ends as well as they do in the 0.5 μm gold electrodes. Thus, we can conclude that DNA can be detected using the impedance spectrum response characteristic. Furthermore, taking advantage of the lower resistances of DNA film at megahertz, DNA-based materials could be used for circuits at frequencies in the order of tens of megahertz. Notice that the electrodes on the gold electrodes have smaller gaps than the electrodes on the platinum electrodes; therefore, gold electrodes are better for bridging. However, as shown in Figs. 5(a) and 6(a), the resistance of DNA is lower on the Pt electrodes because much more DNAs are attached in the parallel direction; even without bridging the gap, the interstitials become short circuits at high frequencies reducing better the resistance for the platinum electrodes.

This work has been supported by the Defense Threat Reduction Agency through the Army Research Office (ARO).

[1] V. Bhalla, R. P. Bajpai, and L. M. Bharadwaj, EMBO Rep. **4**, 442 (2003).
[2] M. A. Lyshevski, IEEE Conference, 2005 [Nanotechnology **1**, 215 (2005)].
[3] E. Ben-Jacob, Z. Hermon, and S. Caspi, Phys. Lett. A **263**, 199 (1999).
[4] C. Ge, J. Liao, W. Yu, and N. Gu, Biosens. Bioelectron. **18**, 53 (2003).
[5] E. Braun, Proceedings of Seventh International Conference on Solid-State and Integrated Circuits Technology, 2004 (unpublished), Vol. 3, pp. 1761–1766.
[6] S. J. Park, T. A. Taton, and C. A. Mirkin, Science **295**, 1503 (2002).
[7] B. Singh, N. S. Sariciftci, J. G. Grote, and F. K. Hopkins, J. Appl. Phys. **100**, 024514 (2006).
[8] G. Subramanyam, E. Heckman, J. Grote, and F. Hopkins, IEEE Microw. Wirel. Compon. Lett. **15**, 232 (2005).
[9] A. J. Steckl, Pit and Quarry **1**, 3 (2007).
[10] E. M. Heckman, J. G. Grote, F. K. Hopkins, and P. P. Yaney, Appl. Phys. Lett. **89**, 181116 (2006).
[11] S. F. Wolf, L. Haines, J. Fisch, J. N. Kremsky, J. P. Dougherty, and K. Jacobs, Nucleic Acids Res. **15**, 2911 (1987).
[12] C. Serge, Electroanalysis **17**, 1701 (2005).
[13] F. F. Chehab and Y. W. Kan, Proc. Natl. Acad. Sci. U.S.A. **86**, 9178 (1989).
[14] E. Laios, P. C. Ioannou, and T. K. Christopoulos, Anal. Chem. **73**, 689 (2001).
[15] S. Bhattacharya, C. Jaewon, S. Lodha, D. B. Janes, A. F. Bonilla, J. Kyung Jae, and G. U. Lee, IEEE-NANO 2003. 2003 Third IEEE Conference [Nanotechnology **2**, 79 (2003)].
[16] L. Zheng, J. P. Brody, and P. J. Burke, Biosens. Bioelectron. **20**, 606 (2004).
[17] Z. G. Yu and X. Song, Phys. Rev. Lett. **86**, 6018 (2001).
[18] P. Tran, B. Alavi, and G. Gruner, Phys. Rev. Lett. **85**, 1564 (2000).
[19] Y. Zhang, R. H. Austin, J. Kraeft, E. C. Cox, and N. P. Ong, Phys. Rev. Lett. **89**, 198102 (2002).
[20] C. Gomez-Navarro, F. Moreno-Herrero, P. J. de Pablo, J. Colchero, J. Gomez-Herrero, and A. M. Baro, Proc. Natl. Acad. Sci. U.S.A. **99**, 8484 (2002).
[21] A. Y. Kasumov, M. Kociak, S. Gueron, B. Reulet, V. T. Volkov, D. V. Klinov, and H. Bouchiat, Science **291**, 280 (2001).
[22] K. H. Yoo, D. H. Ha, J. O. Lee, J. W. Park, J. Kim, J. J. Kim, H. Y. Lee, T. Kawai, and H. Y. Choi, Phys. Rev. Lett. **87**, 198102 (2001).
[23] H. Kitano, K. Ota, and A. Maeda, J. Phys. Soc. Jpn. **75**, 1 (2006).
[24] O. Legrand, D. Cote, and U. Bockelmann, Phys. Rev. E **73**, 031925 (2006).
[25] H. Kleine, R. Wilke, C. Pelargus, K. Rott, A. Puhler, G. Reiss, R. Ros, and D. Anselmetti, J. Biotechnol. **112**, 91 (2004).
[26] A. Rakitin, P. Aich, C. Papadopoulos, Y. Kobzar, A. S. Vedeneev, J. S. Lee, and J. M. Xu, Phys. Rev. Lett. **86**, 3670 (2001).
[27] A. Li, F. Yang, Y. Ma, and X. Yang, Biosens. Bioelectron. **22**, 1716 (2007).
[28] M. Gheorghe and A. Guiseppi-Elie, Biosens. Bioelectron. **19**, 95 (2003).
[29] L. Miao and J. M. Seminario, J. Chem. Phys. **127**, 134708 (2007).
[30] L. Miao and J. M. Seminario, J. Phys. Chem. C **111**, 8366 (2007).
[31] J. A. Seminario, L. M. Yan, and Y. F. Ma, IEEE Trans. Nanotechnol. **5**, 436 (2006).
[32] L. Yan, Y. Ma, and J. M. Seminario, J. Nanosci. Nanotechnol. **6**, 675 (2006).
[33] J. M. Seminario, L. Yan, and Y. Ma, *Chemical and Biological Standoff Detection III*, edited by J. O. Jensen and J. M. Theriault, (SPIE, Bellingham, WA, 2005) Vol. 5995, pp. 230–244.
[34] J. M. Seminario, L. Yan, and Y. Ma, J. Phys. Chem. A **109**, 9712 (2005).
[35] J. M. Seminario, L. Yan, and Y. Ma, Proceedings of IEEE Nanotechnology Conference (unpublished), Vol. 5, pp. 65–68, 2005.
[36] Y. Ma, L. Yan, and J. M. Seminario, Proc. SPIE **5790**, 206 (2005).
[37] J. M. Seminario, Nat. Mater. **4**, 111 (2005).
[38] J. M. Seminario, Proc. SPIE **5411**, 103 (2004).
[39] P. A. Derosa, V. Tarigopula, and J. M. Seminario, *Encyclopedia of Nanoscience and Nanotechnology* (Dekker, New York, 2004).
[40] J. M. Seminario, L. A. Agapito, and H. P. Figueroa, Proceedings of IEEE Nanotechnology Conference, 2002 (unpublished) Vol. 2, pp. 287–290.
[41] J. M. Seminario, L. Yan, and Y. Ma, Proc. IEEE **93**, 1753 (2005).
[42] Microlithographically fabricated interdigitated microsensor electrodes (IMEs) from ABTECH Scientific Inc. (Part No. IAME-co-IME 2-1 Pt, Richmond, VA).
[43] Multimode SPM Instruction Manual, Digital Instruments Veeco Metrology Group, Woodbury, NY, 1999.
[44] S. Tuukkanen, A. Kuzyk, J. J. Toppari, H. Hakkinen, V. P. Hytonen, E. Niskanen, M. Rinkio, and P. Torma, Nanotechnology **18**, 295204 (2007).
[45] L. Desert Cryogenics, TTP-4 Probe Station Operating Guide, Tucson, AZ, 2004.
[46] L. Yokogawa, Operation and Service Manual, Model 4145A Semiconductor Parameter Analyzer, Hewlett-Packard, Palo Alto, CA, 1982.
[47] Tektronix, User Manual TDS5000 series digital phosphor oscilloscopes, Beaverton, OR.
[48] Tektronix, Arbitrary/Function Generators AFG3252, Beaverton, OR.